# Complex SRO isothermal kinetics in quenched Cu–12 at.% Mn assessed by microhardness measurements

A. Varschavsky *, E. Donoso, G. Díaz

*Departamento de Ciencia de los Materiales, Facultad de Ciencias Físicas y Matemáticas, Universidad de Chile, Plaza Ercilla 883, Casilla 1420, Santiago, Chile*

**Abstract**

The isothermal kinetics of the return of short-range-order (SRO) in quenched Cu–12 at.% Mn alloy samples subsequently annealed at various temperatures was analyzed by means of microhardness measurements. An apparent first-order kinetic function is suitable for describing the overall kinetics. Deviations from the straight line in the Arrhenius plot were unequivocally detected. Apparent activation energy values, which lie between those for defect migration of unbound and bound vacancies, approach to that of the unbound ones as annealing temperature is raised. An apparent compensation effect CE was also confirmed. By using an isoconversional equation can be concluded that the degree of conversion is independent of activation energy. The deviation of the isotherms from a formal first-order kinetic mechanistic equation is interpreted in terms of entangled parallel reactions contributed by bound and unbound vacancies. The use of an overall single step rate reaction equation as an operative one, as it was done here, instead of the true rate equation describing a complex process involving multistep reactions is often applied in kinetic analysis.

*Keywords:* Cu–12 at.% Mn; Short-range-order; Kinetics; Microhardness

## 1. Introduction

Much work has already done on CuMn alloys, partly because of great technical interest in the mechanical, electrical and magnetic properties of this alloy system. In recent papers [1,2] we reported calorimetric studies of disperse-short-range-order (DSRO) in Cu–20 at.% Mn [1] and short-range order (SRO) in Cu–12 at.% Mn [2] alloys. In the first state-ordering phenomenon is a process leading to a stable and heterogeneous microstructure. This state has also referred to occur in Cu–γMn concentrated solid solutions [3–5]. It was characterized by the presence of highly ordered particles embedded in a disordered matrix, exhibiting a $Cu_3Mn$ structure [3]. On the contrary, in the second state which has been also reported in other dilute solid solutions [6–10], the short-range-order (SRO) prevailing is characterized by an orderliness of structure which extends over short distances only, in any direction of the alloy system.

In spite of the profuse research work still currently performed on CuMn alloys [11–18], only scarce information exists on SRO behavior in dilute and moderate dilute solid solutions [2,19]. We have chosen for this study a Cu–12 at.% Mn alloy, as it was previously done, which falls outside the possible existing $\gamma'/\gamma''$ phase boundaries [4], and close to the left limit of the enveloping ordered $\varepsilon$ phase domain also reported [20]. In this way the alloy under study exhibit practically SRO only. On the other hand, this alloys concentration is high enough for allowing accurate measurements of ordering effects with most of the experimental techniques usually employed. At this alloy composition it has also been reported the interesting fact that the ordering energies of the first coordination sphere seem to be important as compared with the ordering energies of the first coordination sphere [21].

The SRO-states were produced by: slowly cooling, annealing after quenching from homogenization temperatures, deformation, irradiation with neutrons. Experimentally, many methods can be used to gain information on SRO, e.g. diffuse scattering of X rays or neutrons, transmission electron microscopy, field ion microscopy, Mösbauer spectroscopy, stress induced directional ordering, differential scanning calorimetry (DSC).

Microhardness measurements have proved in the present work to be a useful tool in studying SRO-states behavior,

* Corresponding author.
*E-mail address:* avarscha@cec.uchile.cl (A. Varschavsky).

because here a great accuracy for microstructural changes is combined with a relative great experimental simplicity. In this way it is possible to study extensively the temperature and time dependences of most SRO features. In addition, although research work on ordering phenomenon in Cu–γMn continues [1,2], there are comparatively few studies on the isothermal kinetics of the SRO process from a quantitative treatment of hardness measurements. Besides, no systematic research concerning quantitative evaluation of SRO after quenching and reordering until equilibrium is reached have been reported hitherto particularly by employing microhardness measurements.

Chiefly the main scope of the present work is to analyze for this alloy system, on the basis of some theoretical approaches, kinetic data obtained from microhardness against time dependences for various annealing temperatures after quenching. Special interest will be given to the anomalous behavior exhibited by the apparent activation energy of the ordering process. It will be also searched for other singular kinetic features. An attempt to explain them in terms of the contribution of solute–vacancy complexes will be made.

## 2. Experimental

The alloy studied contained 12 at.% manganese. It was prepared in a Baltzer VSG 10 vacuum induction furnace from electrolytic copper (99.95 wt.%) in a graphite crucible. The ingot was subsequently forged at 923 K to a thickness of 10 mm, pickled with a solution of nitric acid (15% in distilled water) to remove surface oxide, annealed in a vacuum furnace at 1123 K for 36 h to achieve complete homogeneity, and cooled in the furnace to room temperature. It was then cold-rolled to a thickness of 1.5 mm with intermediate annealing periods at 923 K for 1 h. After the last anneal, the material was finally rolled to a thickness of 0.75 mm (50% reduction).

A subsequent heat treatment was performed at 1073 K for 1 h, followed by quenching in a high rate quenching device developed in our laboratory. The quench time was measured with an oscilloscope and estimated in 200 ms. Such a high quench rate was used in order to promote a one-stage ordering process via an excess of free and bound vacancies from the selected quenching temperature. That is, by minimizing defect losses during the quench, sufficient defects in excess are available to reach an equilibrium state of SRO. Otherwise, reordering would involve two stage processes, the first assisted by excess defects and the second by equilibrium defects [1,22,23]. A one-stage ordering process facilitates to visualize the roles of unbound and bound vacancies.

Microhardness measurements were performed in a high accuracy Duramin -1/-2 Struers machine employing a load of 1.96 N during 10 s in specimen discs 0.75 mm in thickness and 6 mm in diameter. Such measurements were made in quenched and subsequently annealed specimens for different times. The annealing temperatures used after quench from 1073 K were 400/425/450/475/500 K. Microhardness has the advantage that early time data can be assessed without difficulty.

## 3. Results and discussion

### 3.1. Hardness measurements and isotherms

The Vickers hardness $H_v$, measured with the Struers Pyramidal Vickers instrument is $H_v = K(P/d^2)$, where $P$ is the load, $d$ the diameter of the indentation and $K$ is the apparatus constant [24,25]. The area $S$ of the indentation is proportional to $d^2$, namely $bd^2$, where $b$ is a geometrical factor. Thus $H_v = Kb\sigma = A\sigma$ being $A$ a constant and $\sigma$ the stress. Since it can be deduced from that strengthening by SRO $\Delta\sigma_{SRO}$ [26] is proportional to the square of the increment in the local order coefficient $(\Delta\alpha)^2$, is turns out that $\Delta\alpha \propto (\Delta\sigma_{SRO})^{1/2} \propto (\Delta H_v)^{1/2}$. It is worth recalling that $\alpha$ is a measure of the SRO states of the alloy. It is now defined $\Delta H_{v\,max} = H_{ve} - H_{vo}$, where $H_{ve}$ is the value of $H_v$ when the equilibrium degree of SRO is reached at the annealing temperature $T_a$, and $H_{vo}$ the value of $H_v$ after the quench. The hardness increment at time $t$ is $\Delta H_v(t) = H_v(t) - H_{vo}$. Therefore, the degree of SRO conversion (or reacted fraction) $y$ at a certain $T_a$ can be stated as

$$y = \left( \frac{H_v(t) - H_{vo}}{H_{ve} - H_{vo}} \right)^{1/2} \quad (1)$$

Each measure of $H_v$ is the average of six indentations and the $\Delta H_v/H_v$ relative error is about 2%. Hardness isotherms are shown in Fig. 1 at the indicated annealing temperatures for the alloy previously quenched from $T_q = 1073$ K. It can be observed that Vickers hardness values increase with time until a constant value is reached for the different annealing temperatures $T_a$ used. These values are indicative that an equilibrium SRO degree is attained in each case. The larger is $T_a$, the shorter is the time spent in reaching equilibrium at $T_a$. Also as $T_a$ decreases, a larger equilibrium degree of order is established as expected [27]. With the aim to perform a quantitative evaluation of SRO kinetics, curves of Fig. 1 were transformed into conversional isotherms by means of Eq. (1). These curves are shown in Fig. 2 for the different annealing temperatures.

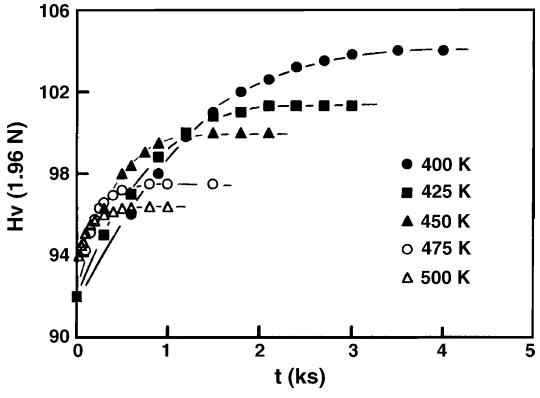


Fig. 1. Vickers microhardness against time at the indicated annealing temperatures. Samples were quenched from a temperature $T_q = 1073$ K. Each data corresponds to the average value of six identations.

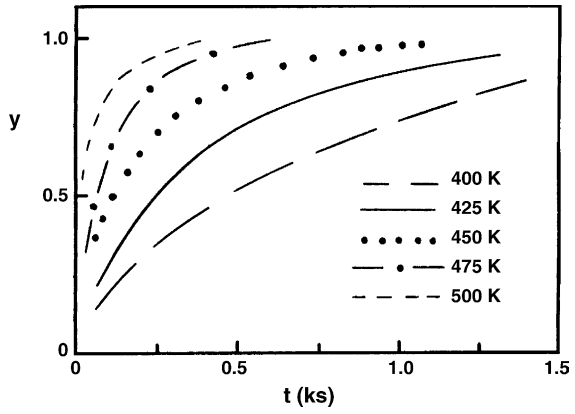


Fig. 2. Reacted fraction (or degree of conversion) processed from microhardness data against time for the indicated annealing temperatures.

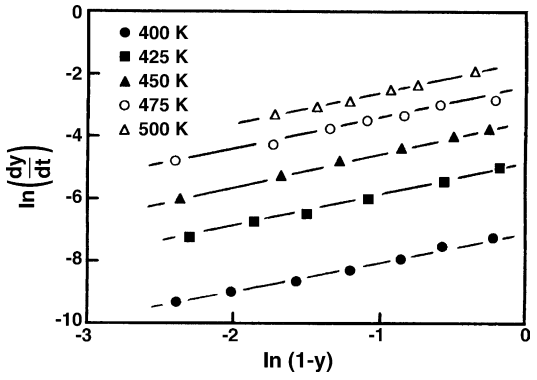


Fig. 3. Logarithm of the reacted fraction rate against the logarithm of the unreacted fraction at the indicated annealing temperatures.

### 3.2. Kinetic reaction function

The rate at which SRO goes from the quenched state to equilibrium at certain annealing temperature d$y$/d$t$ depends on the degree of conversion as well as the temperature of the ordering reaction if an overall single rate equation is considered. Such approximation is often employed in kinetic analysis of systems in which several process takes place. So, under such conditions d$y$/d$t$ can be described as two separate functions of temperature and conversion as

$$\frac{\mathrm{d}y}{\mathrm{d}t} = k(T)f(y) \tag{2}$$

where the first function $k(T)$ is the temperature-dependent and $f(y)$ is a function of the actual degree of order of the sample. For most ordering reactions the temperature dependence is found to be of Arrhenius type although for complex reactions involving more than one step it might be not. Thus, in general the rate constant is given by $k = k_0 \exp(-E/RT)$, where $k_0$ is the apparent pre-exponential factor, $E$ the apparent activation energy, $R$ the gas constant and $T$ is the temperature. For SRO kinetics return, the mechanism—non-invoking method which is a simple extension of homogeneous kinetics is always assumed, so $f(y) = (1-y)^n$, where $n$ is the order of reaction. Therefore the expression:

$$\frac{\mathrm{d}y}{\mathrm{d}t} = k_0 \exp\left(-\frac{E}{RT}\right)(1-y)^n \tag{3}$$

will be used, as profusely have been reported. We will be concerned with finding out the three basic parameters, viz. $k_0$, $E$ and $n$. For correct value of $n$, a plot of

$$\ln\frac{\mathrm{d}y}{\mathrm{d}t} = \ln k + n\ln(1-y) \tag{4}$$

will give a straight line of slope $n$ and intercept $\ln k$. These lines are shown in Fig. 3. Slopes of 0.98/1.05/1.06/0.95/1.04 where measured for the annealing temperatures 400/425/450/475/500 K; hence it is safe to take $n = 1$ for all curves. It has been reported that all deviations from $n = 1$ are due to the annealing out of point defects in high temperature quenched alloys [28,29]. Broken values $1 < n < 2$ were also measured in these references for other alloy conditions. However, $n = 1$ has been generally obtained in most research works concerned with quantitative evaluation of the kinetics of SRO return, as in the present work. This fact indicates that a first-order kinetic function would rule the ordering process provided $k$ follows the Arrhenius equations. Broken values of $n$ must be regarded as effective reaction orders. It is not yet understood why just these values are obtained and what their physical meaning is. The measured rate constant behavior will be analyzed below.

In closing this section it is worth to recall that the derivatives d$y$/d$t$ were measured in Fig. 2 with high accuracy by a geometrical method which not requires previous knowledge of the kinetic function $f(y)$ [30].

### 3.3. Apparent activation parameters

The logarithm of $k$-values obtained from the intercepts of the straight lines of Fig. 3 are plotted against $1/T$ in Fig. 4. It can be observed a deviation of the straight line predicted by the Arrhenius equation. This is an almost certain indication that the observed ordering reaction is a composite one, made up of two or more concurrent reactions differently influenced by temperature [31]. Such results, which will be justified latter on for the alloy under study, should not be considered to

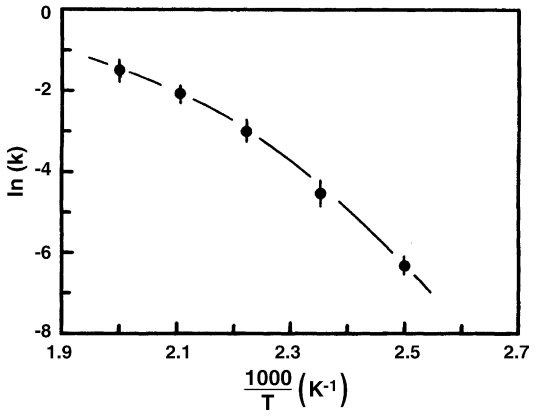


Fig. 4. Arrhenius plot for the experimental apparent rate constant.

be obtained so infrequently [32–37]. Two or more simultaneous processes with different activation energies yield a plot which is concave upwards while consecutive processes are reflected in a plot which is concave downwards [31]. It has also been argumented that apparent activation energy may vary if an incorrect one step mechanistic kinetic function $f(y)$ is used [38]. This is not the present case, since the highest correlation coefficient was obtained for the straight lines shown in Fig. 3 for the kinetic model $R_{1.0}$ according to the code model classification [39], where the subscript number refers to n value, if SRO kinetics can be described only by $R_n$ functions as have been profusely reported in the literature.

The variability of the apparent activation parameters with temperature and/or degree of conversion was extensively discussed recently by Galwey [37,40], concluding that the calculated values of $k_0$ and $E$ for complex reactions using single rate overall reaction kinetics cannot be assumed to provide in general a measure real frequency of occurrence of a single dominant rate controlling chemical or physical step. Even more, application of the Arrhenius equation to solid-state kinetics is now under discussion [37]. Nevertheless apparent activation energies and pre-exponential factors derived from the Arrhenius plot of Fig. 4 will be used. Apparent activation energies, $E$, are measured accurately by the same geometrical procedure as d$y$/d$t$ in Fig. 2 for tangents determination at different temperatures [30]. An apparent particular value of $k_0$ was evaluated from the corresponding apparent activation energy and temperature.

### 3.4. Physical basis for the E = E(T) dependence

The above results are attempted to be analyzed in terms of the simultaneous contributions of free vacancies and solute–vacancy complexes to the temperature dependence of apparent activation parameters. Firstly the contribution of both types of defects to the activation energy is considered. In fact, solute–vacancy binding in Cu–γMn alloys may be important regarding the effective vacancy mobility. In general the binding effect arises from two factors: size factor and electronic factor [41]. The size factor is responsible for the strain field being produced by the size mismatch for oversized solute elements such that the lattice strain so produced is minimized by solute–vacancy atom association. The electronic factor, is considered to be prevalent in the presence of a solute element of valence higher than that of the host element. In the case of Cu–γMn alloys, at least the second factor is present since the Mn valence is higher than that of Cu, being the Mn size slightly smaller. Hence a non-negligible binding energy may arise in a Mn–vacancy complex. A value of binding energy $B = 15.0\,\mathrm{kJ\,mol^{-1}}$ was calculated on average [2,42]. Such a value is considered high enough in that an important fraction of atoms might be bound. For instance, for Cu–12 at.% Mn this less mobile complexes increase the apparent activation energy $E$ for vacancy migration, compared with the calculated value for the activation energy of migration of monovacancies as it will be shown below. Activation energy for monovacancies are estimated as follows since not available data was found. For the present alloy composition, a self-diffusion activation energy $E_{sd} = 186.3\,\mathrm{kJ\,mol^{-1}}$ has been reported [5]. For most copper solid solutions the activation energy for unbound vacancy migration $E_m$ is about $E_m = E_{sd}/2.36$ [43–45], thus $E_m = 78.8\,\mathrm{kJ\,mol^{-1}}$. A migration energy for solute–vacancy complexes, $E_c = 92.8\,\mathrm{kJ\,mol^{-1}}$ was estimated [2]. The apparent activation energy $E$ relates $E_m$ and $E_c$ by [6]

$$\exp\left(-\frac{E}{RT}\right) = \exp\left(-\frac{E_m}{RT}\right)(1-\Psi_b(T)) + \exp\left(-\frac{E_c}{RT}\right)\Psi_b(T) \quad (5)$$

where

$$\Psi_b(T) = \frac{Z\bar{c}\exp\left(\frac{B}{RT}\right)}{1-(Z+1)\bar{c}+2Z\bar{c}\exp\left(\frac{B}{RT}\right)} \quad (6)$$

is termed the equilibrium transfer function [6], $B$ is the solute–vacancy binding energy, $\bar{c}$ the alloy composition and $Z$ the coordination number. Also $\psi_b(T) = c_b/c_t$ in which $c_b$ and $c_t$ are the bound and total vacancy concentrations in thermal-equilibrium. It should be noted that $c_t = c_u + c_b$; $c_u$ is the unbound vacancy concentration. The idea contained in Eq. (5) is that the entire population of vacancies, unbound and bound, is assigned an effective jump frequency which is obtained as weighted sum of simpler jump frequencies describing individual processes. The simpler jump frequencies are given by $\nu_u = \nu_{ou}\exp(-E_m/RT)$ and $\nu_b = \nu_{ob}\exp(-E_c/RT)$. The attempt frequency $\nu_{ou}$ ($=\nu_{ob}$) is considered as a first approximation to be the same for unbound and bound vacancies and also equal to the composite attempt frequency $\nu_{ot}$. Therefore, the effective attempt frequency can be taken as $\nu_{ot} = 12\nu_o\exp(\Delta S_m/R)$, where $\nu_o$ is the Debye frequency and $\Delta S_m$ the activation entropy of migration of free vacancies. Such an assumption is not strictly true [46], hence Eq. (5) must be taken as a first approximation. Furthermore, is has been demonstrated [47] that the formation of solute–vacancy pairs occurs on the quick time scale for vacancy relaxations, and for most purposes the number of such pairs can be assumed to be in equilibrium with the state of chemical order in the alloy. This feature means that although $c_u$ and $c_b$ might decay somewhat during the SRO return, they always will be in dynamic equilibrium obeying the relationship $c_b/c_u = \Psi_b(T)/[1-\Psi_b(T)]$. Vacancy decay while the kinetics of

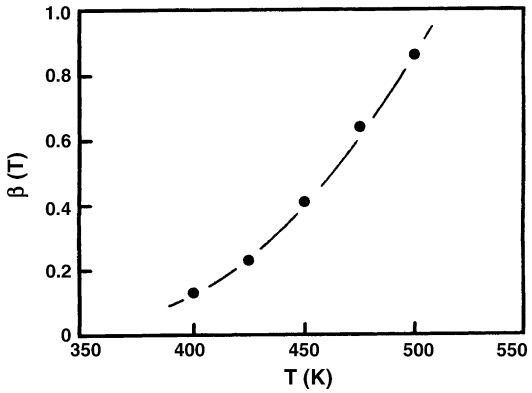


Fig. 5. Weighting factor $\beta(T)$ as a function of temperature.

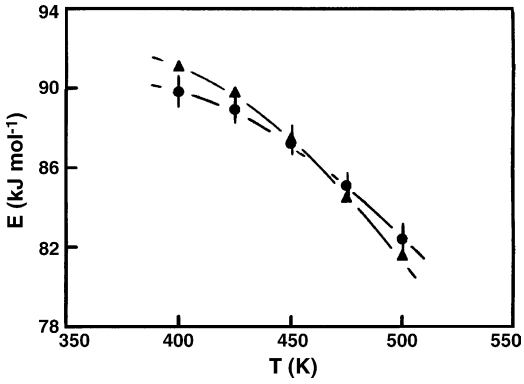


Fig. 6. Calculated (▲) and experimental (●) apparent activation energies against temperature.

SRO process takes place was reported in alloys quenched from low temperatures [29].

In order to have a deeper insight of apparent activation energy behavior $E$ in terms of a linear dependence of $E_m$ and $E_c$, it can be expressed as [2]

$$E = E_c - \beta(T)(E_c - E_m) \tag{7}$$

in which $\beta(T)$ is a temperature-dependent weighting factor. From Eqs. (5) and (7) one gets:

$$\beta(T) = \frac{1}{(E_m - E_c)}\left[RT\left(\ln\frac{1}{(1-\Psi_b(T))\exp\left(-\frac{E_m}{RT}\right)+\Psi_b(T)\exp\left(-\frac{E_c}{RT}\right)}\right) - E_c\right] \tag{8}$$

which is shown in Fig. 5. In this figure also indicates that $\beta(T)$ increases with temperature which means that $E$ is closer to $E_c$ for lower temperatures, thus reflecting a higher contribution of solute–vacancy complexes. On the contrary, for higher temperatures ordering is established by a marked contribution of unbound vacancies. The above findings indicate that the apparent activation energy decrease for increasing temperatures, stems from the fact that the relative unbound vacancy concentration becomes more important as it is expected [48]. The average calculated $E$ values and those measured by geometrical methods in Fig. 4 are compared in Fig. 6. It can be observed that the data points calculated from Eqs. (7) and (8) falls inside the uncertainly bar of $E$ obtained from the slopes of Fig. 4. The very good agreement shown will be also confirmed latter on in connection with the use of an overall single step mechanistic rate equation (Eq. (2)), instead of a true rate equation corresponding to a complex process consisting of two linked parallel reactions as it is the present case, i.e. short-range-order return assisted simultaneously by excess unbound and bound vacancies.

### 3.5. Apparent compensation effect

Compensation effect CE, is the interdependence of apparent Arrhenius parameters, expressed by

$$\ln k_0 = \alpha^* + \beta^* E \tag{9}$$

where $\alpha^*$ and $\beta^*$ are the compensation parameters. CE is found for groups of related rate processes, also for sets of rate data for the same reaction proceeding under different conditions and for alternative calculations based on a single set of original kinetic data. For a compensation effect to be true it must hold that $\alpha^* = \ln k_{iso}$ and $\beta^* = (RT_{iso})^{-1}$, which express that for all sets of ($k_0$, $E$) straight lines, a singular isokinetic point ($k_{iso}$, $T_{iso}$) in the Arrhenius plot exist where all these lines intercept each other. (The theoretical basis of this behavior is still in discussion [49–51].) The compensation effect would be only apparent if the above condition is not fulfilled.

The ($k_0$, $E$) data calculated from Fig. 4 obeys Eq. (9) as shown in Fig. 7, but an isokinetic point ($k_{iso}$, $T_{iso}$) could not be found. The necessity of fulfilling the above relations for $\alpha^*$ and $\beta^*$ is subjected to the definition of CE [52]. It is safe refer the compensation parameters as apparent in the present case. Values of $\alpha^* = -10.35$ and $\beta^* = 0.35 \times 10^{-3}\,\mathrm{mol\,J^{-1}}$ were computed. Work is in progress to search for the physical origin of the linear dependence of $\ln k_0$ and $E$ found here. Such linear dependence reflects that the kinetic function $f(y) = 1 - y$ is a correct choice in this case [39]. It is also useful for assessing the variation of $k_0$ with temperature.

If apparent activation energies are calculated with the present approach formally from $\mathrm{d}\ln k/\mathrm{d}(1/T)$, they differ by a negligible amount from geometrically measured values. In fact, as $k = k_0\exp(-E/RT)$, by using Eqs. (7)–(9) one gets:

$$\frac{\mathrm{d}\ln k}{\mathrm{d}\left(\frac{1}{T}\right)} = \left(\beta^* - \frac{1}{RT}\right)(E_c - E_m)T^2\frac{\mathrm{d}\beta(T)}{\mathrm{d}T} - \frac{E_c - \beta(T)(E_c - E_m)}{R} \tag{10}$$

The first term of Eq. (10) ranges between $2.8 \times 10^2$ and $3.7 \times 10^2$ K for annealing temperatures of 400 and 500 K, which is two orders of magnitude lower, as compared with $1.1 \times 10^4$ and $1.62 \times 10^4$ K for the second one at these temperatures. In closing this section, the calculated and the experimental

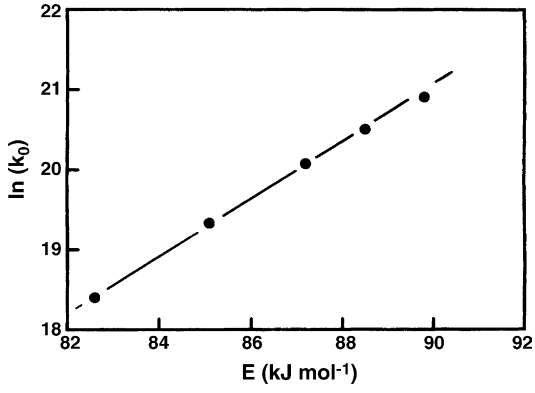


Fig. 7. Logarithm of apparent pre-exponential factor against apparent activation energy showing an eventual compensation effect (CE).

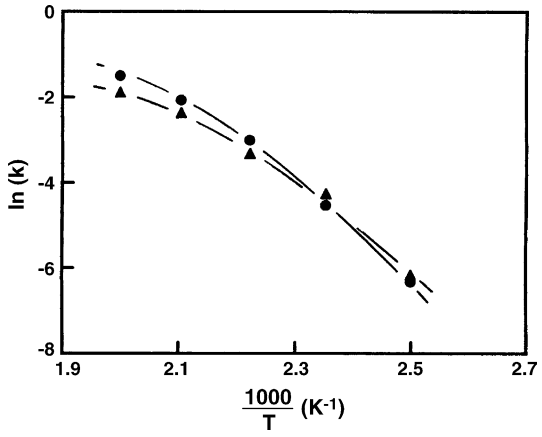


Fig. 8. Arrhenius plots for calculated (▲) and experimental (●) apparent rate constants.

$\ln k$ versus $1/T$ curves are in excellent agreement as shown in Fig. 8.

### 3.6. Isoconversional evaluations

An isoconversional method [53] was applied for checking a possible dependence of $E(T)$ with the conversion degree y in the course of a reaction path. The method was based on the relation

$$\ln\frac{\mathrm{d}y}{\mathrm{d}t} = \ln[k_0(1-y)] - \frac{E}{RT} \tag{11}$$

obtained from Eq. (3) with $n = 1$ as shown in the present case. For a constant $y$-value, $E$ and $k_0$ can be computed by the geometrical measured slope [30], and intercept respectively of the resulting $\ln(\mathrm{d}y/\mathrm{d}t)$ versus $1/T$ curves shown in Fig. 9. These curves show a small departure of straight lines in correspondence with the previously measured values of $E$ and $k_0$. They were plotted for the indicated degrees of conversion. It can be demonstrated geometrically [30] that for a fixed annealing temperature $T_a$, $E$ does not depend of the degree of conversion. Therefore the SRO kinetic process obeys the same kinetic function along the whole reaction path until completion is reached. This finding points to the fact that $f(y) = 1 - y$ is a true conversion function. Activation energies, measured geometrically in these distorted curves,

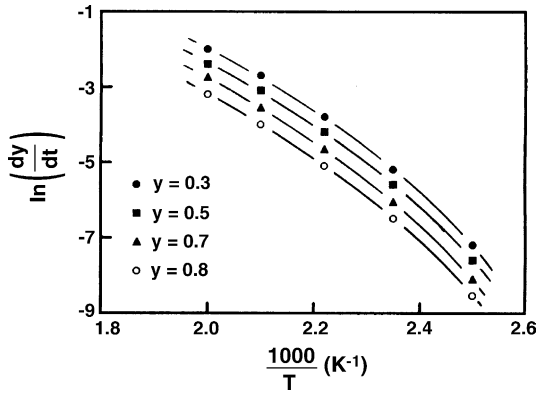


Fig. 9. Logarithm of $(\mathrm{d}y/\mathrm{d}t)$ against the reciprocal of temperature for the indicated degrees of conversion.

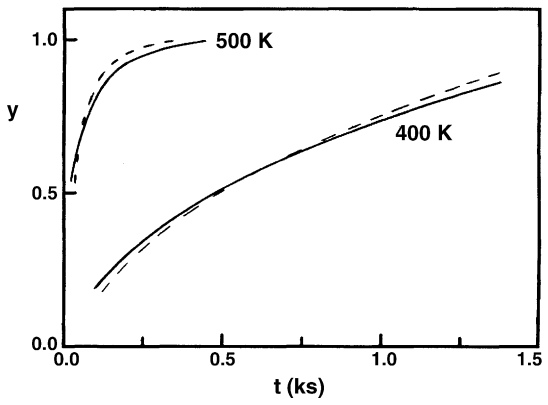


Fig. 10. Calculated (- - -) and experimental (—) reacted fractions against time for the two indicated annealing temperatures.

are almost equal than those measured previously and are not numerically compared for brevity sake.

### 3.7. Prediction of the isotherms y by using the apparent CE parameters and the E = E(T) dependence

The isotherms calculated from all above collected data can be then represented by the apparent first-order kinetic law:

$$y = 1 - \exp(-kt)$$

where the apparent rate constant reads:

$$k = \exp(\alpha^* + \beta^* E)\exp\left(-\frac{E}{RT}\right)$$

where $E$ is obtained from Eq. (7).

It is shown in Fig. 10 an excellent correspondence between the calculated isotherms and those of Fig. 2, for the indicated temperatures.

It should however emphasized that the overall kinetic model here presented might be significant to the ordering kinetic process because it was able to describe individual identified reactions representing two parallel simultaneous processes by a single rate process. Unless systems specific analytical methods, capable of distinguishing individual contributions from two or more processes are applied, this approximation to rate analysis often used cannot be generally successful in measuring the yields from each participating reaction in composite measurements containing contributions from two or more substantially overlapping reactions. Product yield from consecutive or concurrent parallel reactions should be strictly treated by methods suitable for complex reactions [54]. Our successfully close description of the present SRO kinetic process using an overall based kinetic model might stems partially from the close values of the activation energies for migration of solute–vacancy complexes and free vacancies, and from the independence of the apparent activation energy of the conversion degree. The true rate equation required to describe both one-stage and two-stage ordering processes as influenced by bound vacancies is now under study.

## 4. Concluding remarks

The isothermal kinetics of SRO return of the studied alloy could be represented satisfactory by an overall kinetic function based in a first-order mechanistic model. It was inferred that apparent activation energy lies in between the activation energies of unbound and bound vacancies approaching the first one as temperature is raised. The pre-exponential factor correlates the effective activation energy through an apparent compensation effect. By using an isoconversional equation it can be concluded that the degree of conversion is independent of activation energy. The deviation of the rate constant from Arrhenius behavior suggest that a complex process where the entangled simultaneous contribution of solute–vacancy complexes and free vacancies is acting through parallel reactions. An overall kinetic model, as it was developed here is often employed as an operative one instead of the true multistep kinetic equation to which the process strictly obeys.

## Acknowledgements

The authors wish to thank the Fondo Nacional de Desarrollo Cientifico y Tecnológico (FONDECYT) for financial support, Project No. 1040795 and to the Facultad de Ciencias Físicas y Matemáticas de la Universidad de Chile for the facilities given to undertake this research work.

## References

[1] A. Varschavsky, E. Donoso, J. Therm. Anal. Cal. 76 (2004) 853.
[2] E. Donoso, G. Díaz, A. Varschavsky, J. Therm. Anal. Cal. 81 (2005) 425.
[3] H. Warlimont, K. Bernecker, R. Luck, Z. Metallk. 62 (1971) 816.
[4] R. Reishsner, W. Pfeiler, J. Phys. Chem. Solids 46 (1985) 1431.
[5] W. Pfeiler, Acta Metall. 36 (1988) 2417.
[6] A. Varschavsky, G. Díaz, E. Donoso, Mater. Sci. Eng. A 369 (2004) 1.
[7] E. Donoso, A. Varschavsky, Mater. Sci. Eng. A 369 (2004) 10.
[8] A. Varschavsky, E. Donoso, J. Therm. Anal. Cal. 73 (2003) 167.
[9] A. Varschavsky, E. Donoso, J. Therm. Anal. Cal. 65 (2001) 185.
[10] A. Varschavsky, E. Donoso, J. Therm. Anal. Cal. 63 (2001) 397.
[11] A. Varschavsky, E. Donoso, Mater. Lett. 1 (1997) 329.
[12] O. Engler, Acta Mater. 49 (2001) 1237.
[13] O. Engler, Acta Mater. 48 (2001) 4827.
[14] Q.Y. Pan, D. Huang, X. Lind, Y.H. Zhou, G.L. Shang, Mater. Res. Bull. 33 (1998) 1621.
[15] Q.Y. Pan, D. Huang, X. Lin, Y.H. Zhou, J. Cryst. Growth 181 (1997) 109.
[16] H. Roelofs, B. Schonfeld, G. Kostorz, W. Buhrer, J.L. Robertson, P. Zschack, G.E. Lee, Acta Metall. 34 (1996) 139.
[17] H. Roelofs, B. Schonfed, G. Kostorz, W. Buhrer, Phys. Stat. Sol. (b) 187 (1995) 31.
[18] A. Nortmann, Ch. Schwink, Scripta Metall. Mater. 33 (1995) 369.
[19] A. Varschavsky, E. Donoso, Mater. Lett. 31 (1997) 239.
[20] P.R. Subromanian, D.J. Chakrabarty, D.E. Laughlin (Eds.), Phase Diagrams of Binary Copper Alloys, ASM International, Monograph Series on Alloy Phase Diagrams, Ohio, 1994, p. 253.
[21] T.M. Harders, T.J. Hicks, J.H. Smith, J. Phys. F 13 (1983) 1262.
[22] A. Varschavsky, E. Donoso, Mater. Sci. Eng. A 212 (1991) 95.
[23] A. Varschavsky, E. Donoso, Thermochim. Acta 203 (1992) 391.
[24] N. Bouzroura, M. Kadi-Hanif, Phil. Mag. Lett. 84 (2004) 87.
[25] H.P. Stüwe, A.F. Padelha, F. Siciliano Jr., Mater. Sci. Eng. A 333 (2002) 361.
[26] C.H. Cáceres, A. Blanke, Phys. Stat. Sol. (a) 194 (2002) 147.
[27] W. Pfeiler, Acta Metall. 36 (1988) 2417.
[28] W. Col, R. Scheffel, H. Heidsiek, K. Lücke, Acta Metall. 31 (1983) 1895.
[29] A. Bartels, C.M.R. Kemkes, L. Lucke, Acta Metall. 33 (1985) 1887.
[30] G. Moretti (Ed.), Mathematic Methods of Physics, Coni, Buenos Aires, Argentina, 1960, p. 47 (in Spanish).
[31] J.R. Mullet, Quart. Rev. 18 (1964) 227.
[32] S. Vyazovkin, Int. Rev. Phys. Chem. 19 (2000) 45.
[33] S. Vyazovkin, N. J. Chem. 24 (2000) 913.
[34] M.C. Ball, L. Portwood, J. Therm. Anal. 41 (1994) 347.
[35] P. O'Brien, V. Patel, J. Chem. Soc., Dalton Trans. (1982) 1407.
[36] J. Sestak, Heat Thermal Analysis and Society, Nucleus H.K., Hradec Kralove, Czech Republic, 2004, p. 213.
[37] A. Galwey, M. Brown, Thermochim. Acta 386 (2002) 91.
[38] J. Sèsták, Thermophysical Properties of Solids, Elsevier, Amsterdam, 1984, p. 204.
[39] P. Budrugeal, E. Segal, J. Therm. Anal. Cal. 56 (1999) 835.
[40] A. Galwey, Thermochim. Acta 399 (2003) 1.
[41] A.K. Mukhopadhyay, G.I. Shiflet, E.A. Starke Jr., Scripta Metall. Mater. 24 (1990) 307.
[42] S. Ogbilen, M.M. Flower, Acta Metall. 37 (1989) 2993.
[43] J. Andries, W.G. Boonand, S. Radelaar, Phys. Lett. 38A (1972) 459.
[44] E. Balanzat, J. Hillairet, J. Phys. F: Met. Phys. 11 (1981) 1977.
[45] T. Eguchi, Y. Tomokiyo, C. Kinoshita, J. Phys. 38 (1977) 7–382.
[46] C. Zener, J. Appl. Phys. 22 (1950) 372.
[47] B. Fultz, in: J. Chen, V.K. Vasudevan (Eds.), Kinetics of Ordering Transformations in Metals, The Minerals, Metals and Materials Society, Warrendale, PA, 1992, p. 21.
[48] D.V. Ragone, Thermodynamics of Materials, vol. 2, Wiley, New York, 1995, p. 73.
[49] A. Galwey, Thermochim. Acta 294 (1997) 205.
[50] A. Galwey, Thermochim. Acta 407 (2003) 93.
[51] A. Galwey, Thermochim. Acta 294 (2004) 205.
[52] M.P. Suárez, A. Palermo, C.M. Aldao, J. Therm. Anal. 41 (1994) 807.
[53] P. Simon, J. Therm. Anal. Cal. 76 (2004) 123.
[54] A.K. Burnham, R.L. Braun, T.T. Coburn, E.I. Sanvik, D.J. Curry, B.J. Schmidt, R.A. Noble, Energy Fuels 10 (1996) 49.